The effect of anions in the synthesis and structure of pyrazolylamidino copper(II) complexes

Chang-Chih Hsieh,[b] Po-Kuang Liao,[a] Chia-Wei Chen,[a] Ming-Hsi Chiang[b,c] and Yih-Chern Horng[a]*

[a] Department of Chemistry, National Changhua University of Education, Changhua 50058, Taiwan

[b] Institute of Chemistry, Academia Sinica, Taipei 11528, Taiwan

[c] Department of Medicinal and Applied Chemistry, Kaohsiung Medical University, Kaohsiung 80708, Taiwan

* Email: ychorng@cc.ncue.edu.tw

Electronic Supporting Information

Table of Contents

Supplementary Tables and Figures

Table S1. The summary of crystallographic data for the complexes **1**~**3**.

	1	**2**	**3**
formula	C10H14Cl2CuN6O8	C12H18Cl2CuN6O8	C10H14Cl4Cu2N6
fw	480.71	508.76	487.17
temp, K	150(2) K	150(2) K	150(2) K
cryst syst	Monoclinic	Monoclinic	Triclinic
space group	C2/c	$P2_1/n$	P-1
a, Å	15.9429(8)	7.0614(3)	8.279(3)
b, Å	6.0099(3)	15.8795(6)	9.550(3)
c, Å	18.4308(9)	8.9357(3)	11.678(4)
α, º	90	90	94.69(2)
β, °	93.165(3)	108.1762(19)	104.15(2)
γ, º	90	90	106.77(3)
Volume, $Å^3$ / *Z*	1763.26(15) / 4	951.98(6) / 2	845.6(5) / 2
Density (cald.), Mg/m^3	1.811	1.775	1.913
Absorption coefficient, mm^{-1}	1.596	1.484	3.149
crystal size, mm	0.12 x 0.10 x 0.06	0.13 x 0.06 x 0.02	0.08 x 0.08 x 0.06
θ range, deg	2.213 to 28.726	2.565 to 28.773	2.258 to 28.280
no. of reflns collected	12158	11225	8038
no. of indep reflns	2275	2474	4066
max. and min. trans	0.910 and 0.832	0.971 and 0.830	0.810 and 0.754
no. of data /restraints /params	2275 / 0 / 129	2474 / 0 / 134	4066 / 0 / 201
goodness-of-fit on F^2	1.029	1.479	0.797
final *R* indices [$I>2\sigma(I)$] R_1[a], wR_2[b]	0.0337, 0.0750	0.0306, 0.0587	0.0546, 0.1453
R indices (all data), R_1[a] ,wR_2[b]	0.0373, 0.0774	0.0343, 0.0598	0.1123, 0.1790
largest diff. peak and hole, e $Å^{-3}$	0.436 and -0.585	0.540 and -0.456	1.896 and -0.895

[a] $R_1 = \Sigma \left| F_0 \right| - \left| F_c \right| / \Sigma \left| F_0 \right|$

[b] $wR_2 = [\Sigma[\omega(F_0^2 - F_c^2)^2] / \Sigma[\omega(F_0^2)^2]]^{1/2}$

Table S2. The summary of crystallographic data for the complexes **4**~**6**.

	4	**5**	**6**
formula	C6H9Cl2CuN3	C16H22Cl4Cu2N10O8	C18H26Cl4Cu2N10O8
fw	257.61	751.31	779.38
temp, K	150(2)	150(2)	150(2) K
cryst syst	Monoclinic	Monoclinic	Monoclinic
space group	$P2_1/n$	$P2_1/n$	$P2_1/c$
a, Å	8.4981(3)	6.8239(3)	6.6960(5)
b, Å	6.8635(3)	22.2246(12)	14.7680(11)
c, Å	16.2694(6)	9.5718(4)	14.4998(10)
α, º	90	90	90
β, °	103.120(2)	110.437(3)	93.504(4)
γ, º	90	90	90
Volume, $Å^3$ / *Z*	924.17(6) / 4	1360.27(11) / 2	1431.15(18) / 2
Density (cald.), Mg/m^3	1.851	1.834	1.809
Absorption coefficient, mm^{-1}	2.887	2.018	1.922
crystal size, mm	0.34 x 0.18 x 0.01	0.35 x 0.12 x 0.04	0.38 x 0.04 x 0.02
θ range, deg	2.504 to 28.692	2.449 to 28.703	1.970 to 28.753
no. of reflns collected	9864	14575	17360
no. of indep reflns	2391	3492	3650
max. and min. trans	0.972 and 0.540	0.924 and 0.539	0.963 and 0.529
no. of data /restraints /params	2391 / 0 / 110	3492 / 0 / 182	3650 / 0 / 191
goodness-of-fit on F^2	0.670	1.054	1.047
final *R* indices [$I>2\sigma(I)$] R_1[a], wR_2[b]	0.0306, 0.0859	0.0323, 0.1272	0.0607, 0.1598
R indices (all data), R_1[a] ,wR_2[b]	0.0453, 0.0982	0.0375, 0.1320	0.0675, 0.1641
largest diff. peak and hole, e $Å^{-3}$	0.579 and -0.528	0.427 and -0.746	1.918 and -0.711

[a] $R_1 = \Sigma \left| F_0 \right| - \left| F_c \right| / \Sigma \left| F_0 \right|$

[b] $wR_2 = [\Sigma[\omega(F_0^2 - F_c^2)^2] / \Sigma[\omega(F_0^2)^2]]^{1/2}$

Table S3. The summary of crystallographic data for complexes **7**~**9**.

	7	**8**	**9**
formula	C10H14B2CuF8N6	C12H18B2CuF8N6	C16H22B2Cl2Cu2F8N10
fw	455.43	483.48	726.06
temp, K	150(2)	150(2)	150(2)
cryst syst	Monoclinic	Monoclinic	Monoclinic
space group	C2/c	$P2_1/c$	$P2_1/n$
a, Å	15.5827(7)	6.2314(3)	6.8088(6)
b, Å	5.9982(3)	19.6874(8)	21.937(2)
c, Å	18.2326(8)	8.2359(4)	9.5062(9)
α, º	90	90	90
β, °	92.341(3)	108.692(3)	110.098(6)
γ, º	90	90	90
Volume, $Å^3$ / *Z*	1702.75(14) / 4	957.09(8) / 2	1333.5(2) / 2
Density (cald.), Mg/m^3	1.777	1.678	1.808
Absorption coefficient, mm^{-1}	1.373	1.227	1.880
crystal size, mm	0.30 x 0.04 x 0.02	0.10 x 0.02 x 0.02	0.20 x 0.09 x 0.09
θ range, deg	2.236 to 28.728	2.069 to 28.742	1.857 to 28.709
no. of reflns collected	10949	12644	14776
no. of indep reflns	2201	2472	3422
max. and min. trans	0.973 and 0.683	0.976 and 0.887	0.730 and 0.522
no. of data /restraints /params	2201 / 0 / 125	2471 / 0 / 134	3422 / 0 / 182
goodness-of-fit on F^2	0.869	0.961	1.089
final *R* indices [$I>2\sigma(I)$] R_1[a], wR_2[b]	0.0344, 0.0862	0.0383, 0.1038	0.0555, 0.1557
R indices (all data), R_1[a] ,wR_2[b]	0.0457, 0.0941	0.0571, 0.1145	0.0767, 0.1670
largest diff. peak and hole, e $Å^{-3}$	0.568 and -0.390	0.400 and -0.503	1.234 and -0.820

[a] $R_1 = \Sigma \left| F_0 \right| - \left| F_c \right| / \Sigma \left| F_0 \right|$

[b] $wR_2 = [\Sigma[\omega(F_0^2 - F_c^2)^2] / \Sigma[\omega(F_0^2)^2]]^{1/2}$

Table S4. The summary of crystallographic data for complex **10** and $[Cu(pzH)_4(BF_4)_2]$.

	10	$[Cu(pzH)_4(BF_4)_2]$
formula	C18H26B2Cl2Cu2F8N10	C12H16B2CuF8N8
fw	754.11	509.49
temp, K	150(2)	150(2)
cryst syst	Monoclinic	Monoclinic
space group	$P2_1/c$	C2/c
a, Å	6.6757(4)	14.0051(8)
b, Å	14.7202(8)	9.8734(5)
c, Å	14.3589(8)	15.5093(9)
α, º	90	90
β, °	93.853(3)	114.108(3)
γ, º	90	90
Volume, $Å^3$ / *Z*	1407.83(14) / 2	1957.54(19) / 4
Density (cald.), Mg/m^3	1.779	1.729
Absorption coefficient, mm^{-1}	1.784	1.208
crystal size, mm	0.18 x 0.06 x 0.06	0.15 x 0.04 x 0.04
θ range, deg	1.984 to 28.868	2.607 to 28.754
no. of reflns collected	19931	12837
no. of indep reflns	3653	2545
max. and min. trans	0.941 and 0.838	0.953 and 0.840
no. of data /restraints /params	3653 / 0 / 191	2545 / 0 / 142
goodness-of-fit on F^2	0.851	1.001
final *R* indices [$I>2\sigma(I)$] $R_1{}^a$, $wR_2{}^b$	0.0354, 0.1029	0.0435, 0.1635
R indices (all data), $R_1{}^a$,$wR_2{}^b$	0.0392, 0.1059	0.0528, 0.1805
largest diff. peak and hole, e $Å^{-3}$	0.880 and -0.543	1.384 and -0.739

[a] $R_1 = \Sigma \left| F_0 \right| - \left| F_c \right| / \Sigma \left| F_0 \right|$

[b] $wR_2 = [\Sigma[\omega(F_0^2 - F_c^2)^2] / \Sigma[\omega(F_0^2)^2]]^{1/2}$

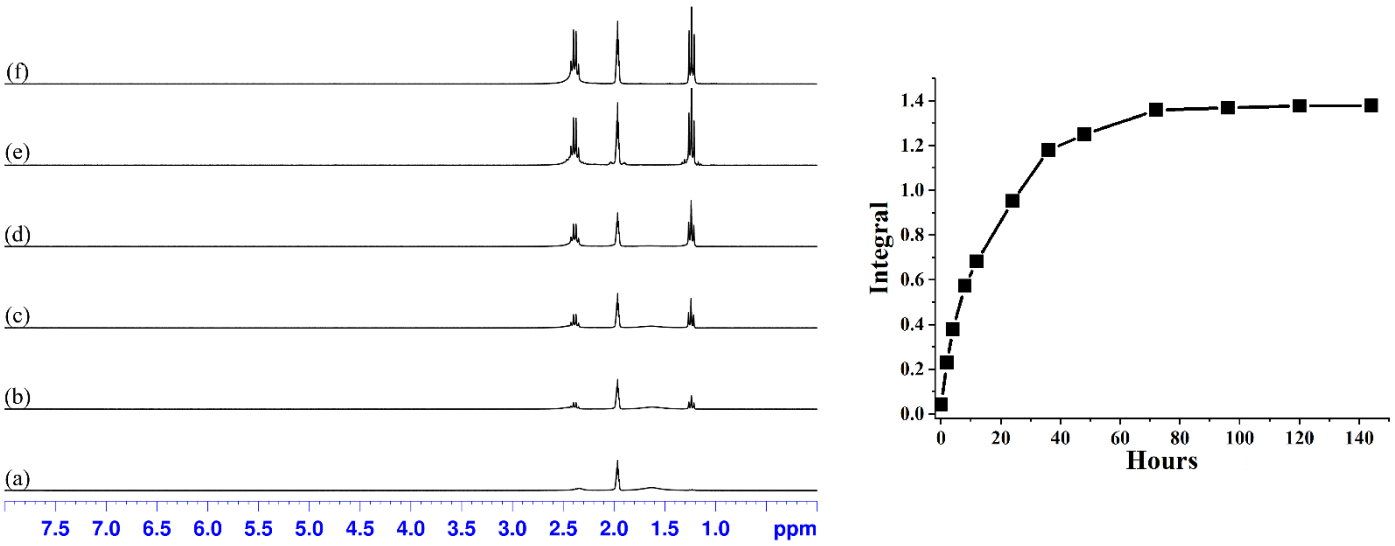

Figure S1. The *in situ* time-dependent ^{1}H NMR experiments of nitrile exchange reaction, which converts compound **2** to compound *d*$_6$-**1**, at 298 K in CD_3CN (1.95 ppm): (a) 0 hr, (b) 4 hrs, (c) 12hrs, (d) 36 hrs, (e) 72 hrs, (f) 144 hrs (left). The time-dependent yield of *d*$_6$-**1** from **2** in *in situ* ^{1}H NMR experiments at 298 K in CD_3CN (right). The integration is based on the peaks at 1.2 ppm (CH_3CH_2CN).

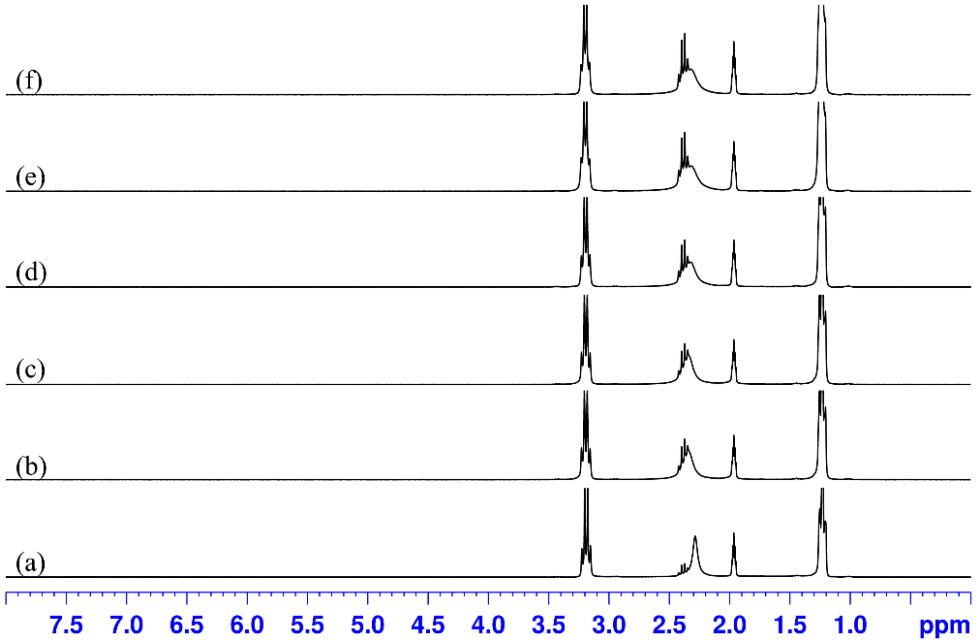

Figure S2. The substitution reaction of compound **2** reacted with 1 equiv. Et_4NCl in *in situ* time-dependent ^{1}H NMR studies in CD_3CN (1.95 ppm) at 298 K, (a) 5 mins, (b) 2 hrs, (c) 4 hrs, (d) 8 hrs, (e) 24 hrs, (f) 72 hrs. The peaks at 1.3 and 3.2 ppm are the ethyl group from $[Et_4N]^+$, and the broad peak at 2.3 ppm is H_2O.

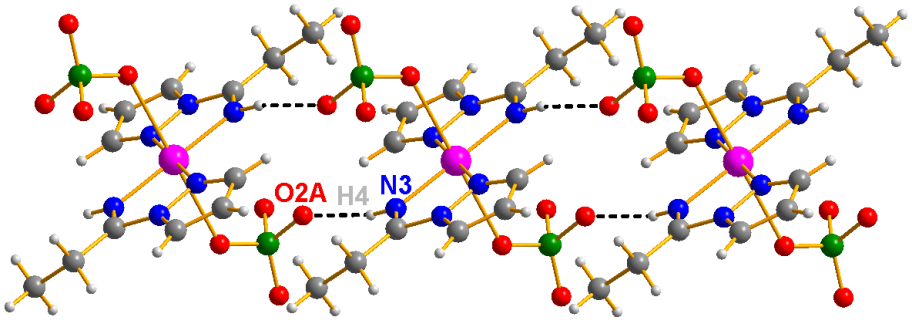

Figure S3. Stair-like one-dimensional polymer of **2** with black dash lines showing the NH···O hydrogen-bond interactions. Only the major component is shown. N3···O2A = 3.0024(33) Å, H4···O2A = 2.1253(28) Å, N3-H4···O2A = 174.3°. Symmetry code: A 1+x, y, z.

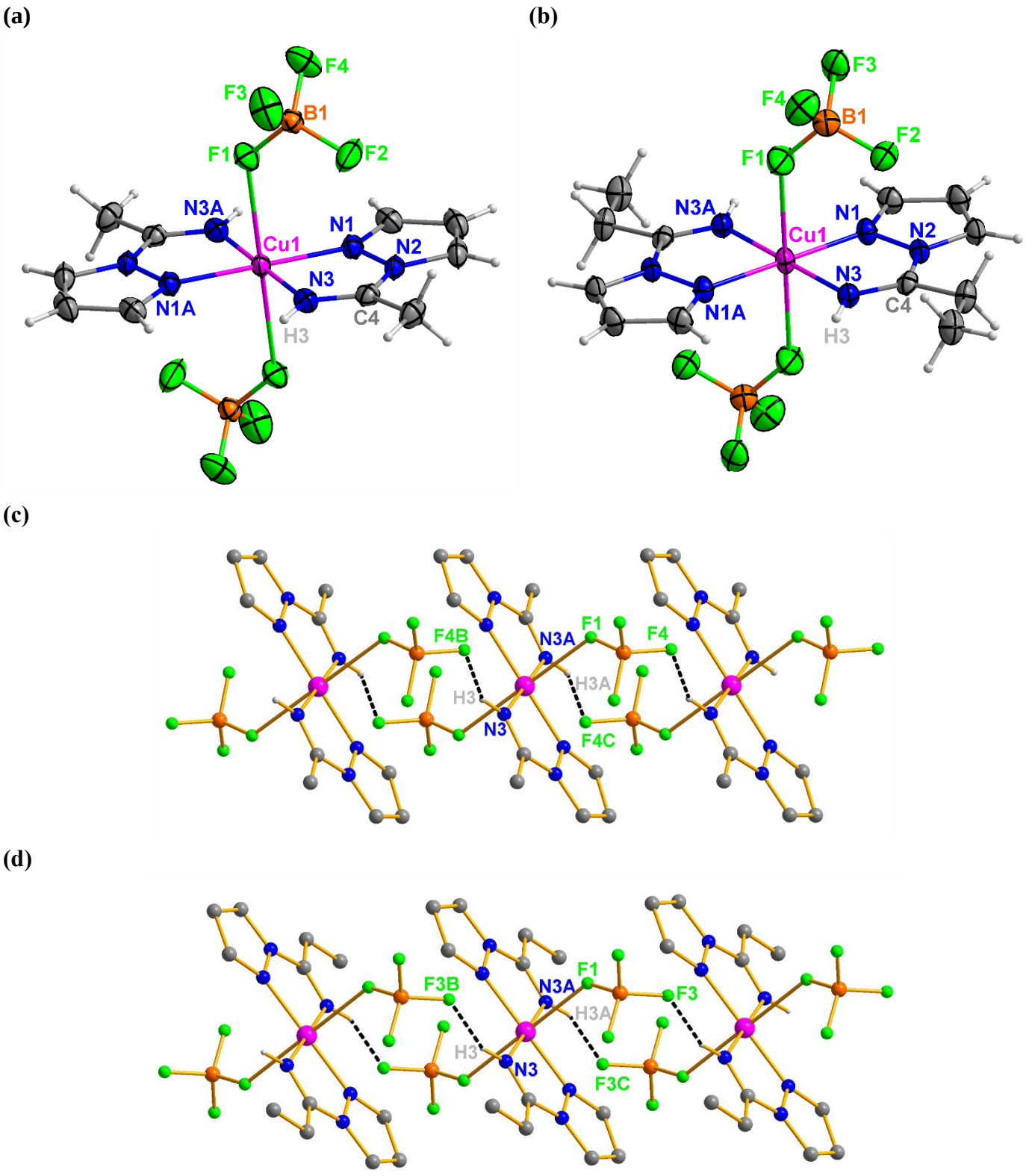

Figure S4. ORTEP style representation of **7** (a) and **8** (b). Thermal ellipsoids are drawn at the 35 % probability level. Stair-like one-dimensional polymer of **7** (c) and **8** (d) with black dash lines showing the NH···F hydrogen-bond interactions. Only the major component is shown. Hydrogen atoms bound to carbon atoms are omitted for clarity. N3···F4B = 2.8932(26) Å, H3···F4B = 2.0916(18) Å, N3-H3···F4B = 151.1(1)° for **7**; N3···F3B = 2.9740(19) Å, H3···F3B = 2.1405(12) Å, N3-H3···F3B = 157.8(1)° for **8**. Symmetry code: A 2-x, 2-y, 1-z for **7** and 1-x, 1-y, 1-z for **8**; B x, 1+y, z for **7** and -1+x, y, z for **8**; C 2-x, 1-y, 1-z.

Table S5. Selected bond lengths [Å] and angles [°] for complex **7** and **8**.[a]

	7	**8**
Cu1-N1	1.9728(17)	1.9777(18)
Cu1-N3	1.9710(18)	1.9853(18)
Cu1-F1	2.5680(14)	2.4758(14)
N3-C4	1.270(3)	1.265(3)
N2-C4	1.392(3)	1.402(3)
N1-Cu1-N3	80.37(8)	80.55(7)
N1-Cu1-N3A	99.63(8)	99.45(8)
N1-Cu1-F1	93.70(6)	91.14(7)
N3-Cu1-F1	88.64(6)	87.83(6)
N3A-Cu1-F1	91.37(6)	92.17(6)
N1A-Cu1-F1	86.30(6)	88.86(7)

[a] Symmetry code: A= 2-x, 2-y, 1-z for **7** and 1-x, 1-y, 1-z for **8**.

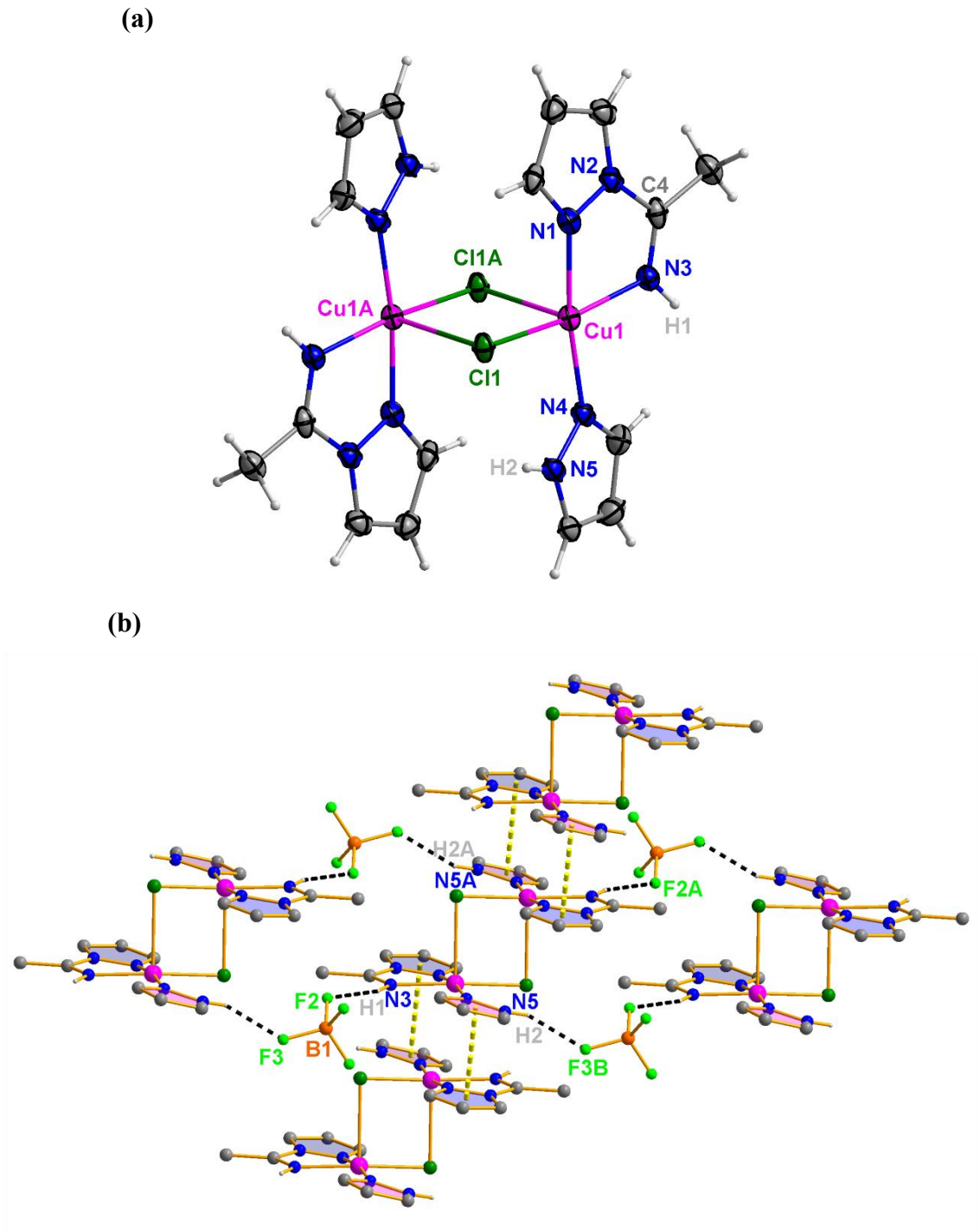

Figure S5. (a) ORTEP style representation of **9**. Thermal ellipsoids are drawn at the 35 % probability level. The counterions (BF_4^-) are omitted for clarity. (b) Two-dimensional packing diagram showing the hydrogen bonding (black dash lines) and π···π (yellow dash lines) interactions. Only the major component is shown. Hydrogen atoms bound to carbon atoms are omitted for clarity. N3···F2 2.8744(44) Å, H1···F2 2.0414(28) Å, N3-H1···F2 157.6(2)°; N5···F3B 2.8042(44) Å, H2···F3B 2.0703(26) Å, N5-H2···F3B 140.3(2)°. The distance between the centroids of bound pzH and L^{Me} pz moiety of nearby molecules is 3.8377(3) Å. Symmetry code: A -x, 2-y, 2-z; B x, y, 1+z.

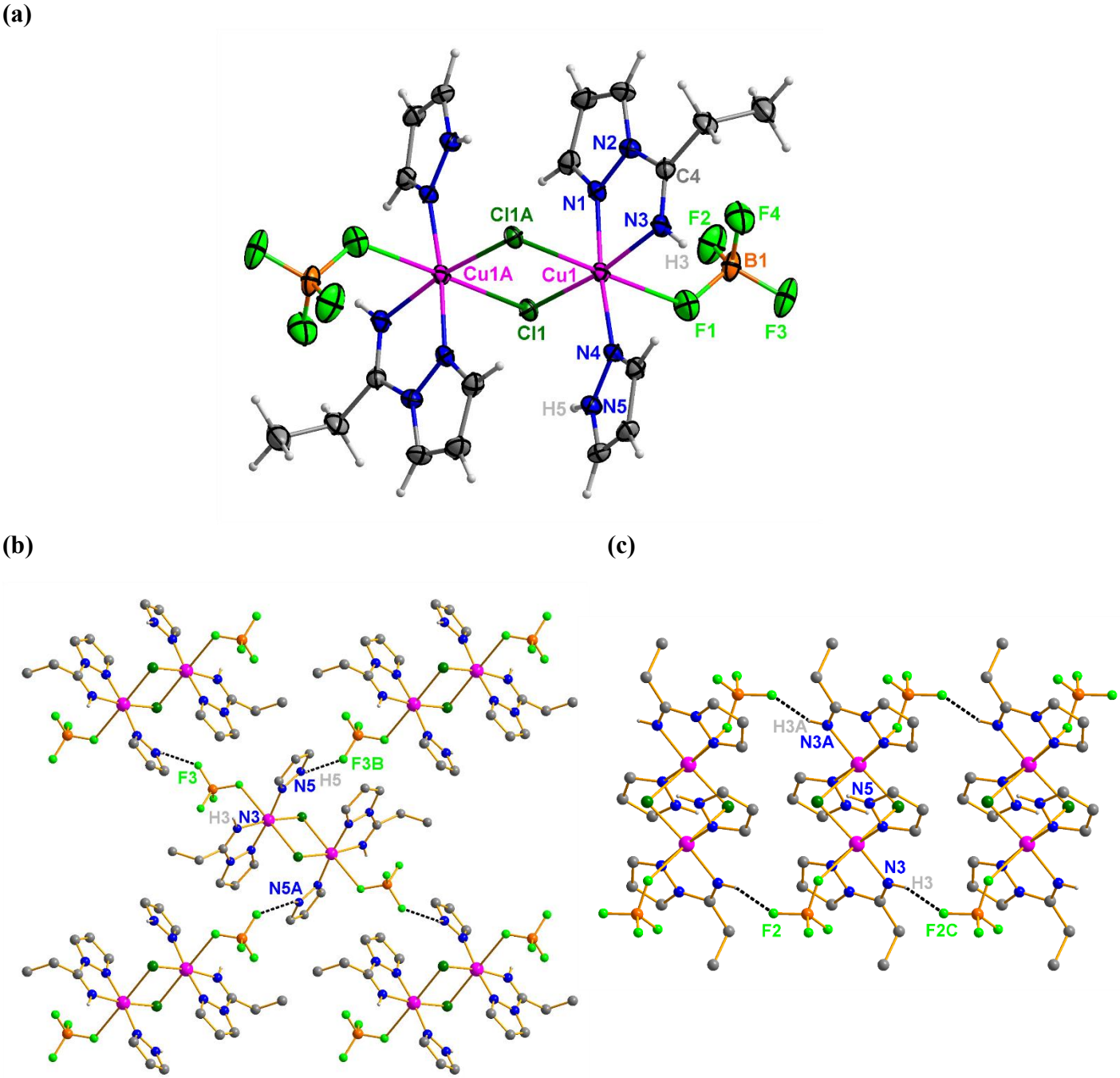

Figure S6. (a) ORTEP style representation of **10**. Thermal ellipsoids are drawn at the 35 % probability level. Packing diagrams are depicted along bc plane (b) and along ac plane (c) with black dash lines showing the NH···F hydrogen-bond interactions. Only the major component is shown. Hydrogen atoms bound to carbon atoms are omitted for clarity. N5···F3B 2.9047(29) Å, H5···F3B 2.2062(21) Å, N5-H5···F3B 136.1(1)°; N3···F2C 2.8905(29) Å, H3···F2C 2.0402(21) Å, N3-H3···F2C 162.0(1)°. Symmetry code: A 1-x, -y, 1-z; B x, 0.5-y, -0.5+z; C 1+x, y, z.

Table S6. Bond lengths [Å] and angles [°] for complex **9** and **10**.[a]

	9	**10**
Cu1-N1	1.992(3)	1.970(2)
Cu1-N3	2.001(3)	2.011(2)
Cu1-N4	1.972(3)	1.971(2)
Cu1-Cl1	2.2631(10)	2.2685(6)
Cu1-Cl1A	2.7468(11)	2.8339(7)
N1-N2	1.359(4)	1.360(3)
N2-C4	1.409(5)	1.400(3)
N3-C4	1.269(5)	1.263(3)
N4-N5	1.348(4)	1.352(3)
Cu1-F1		2.724(2)
N1-Cu1-N3	79.41(12)	79.63(9)
N1-Cu1-Cl1	91.18(9)	91.26(6)
N1-Cu1-Cl1A	92.71(9)	91.84(6)
N3-Cu1-N4	95.94(12)	96.50(9)
N3-Cu1-Cl1A	91.16(9)	85.04(6)
N4-Cu1-Cl1	92.98(9)	92.72(6)
N4-Cu1-Cl1A	94.02(10)	91.85(6)
Cl1-Cu1-Cl1A	92.94(3)	93.52(2)
Cu1-Cl1-Cu1A	87.06(3)	86.48(2)

[a] Symmetry code: A= -x, 2-y, 2-z for **9**; 1-x, -y, 1-z for **10**.

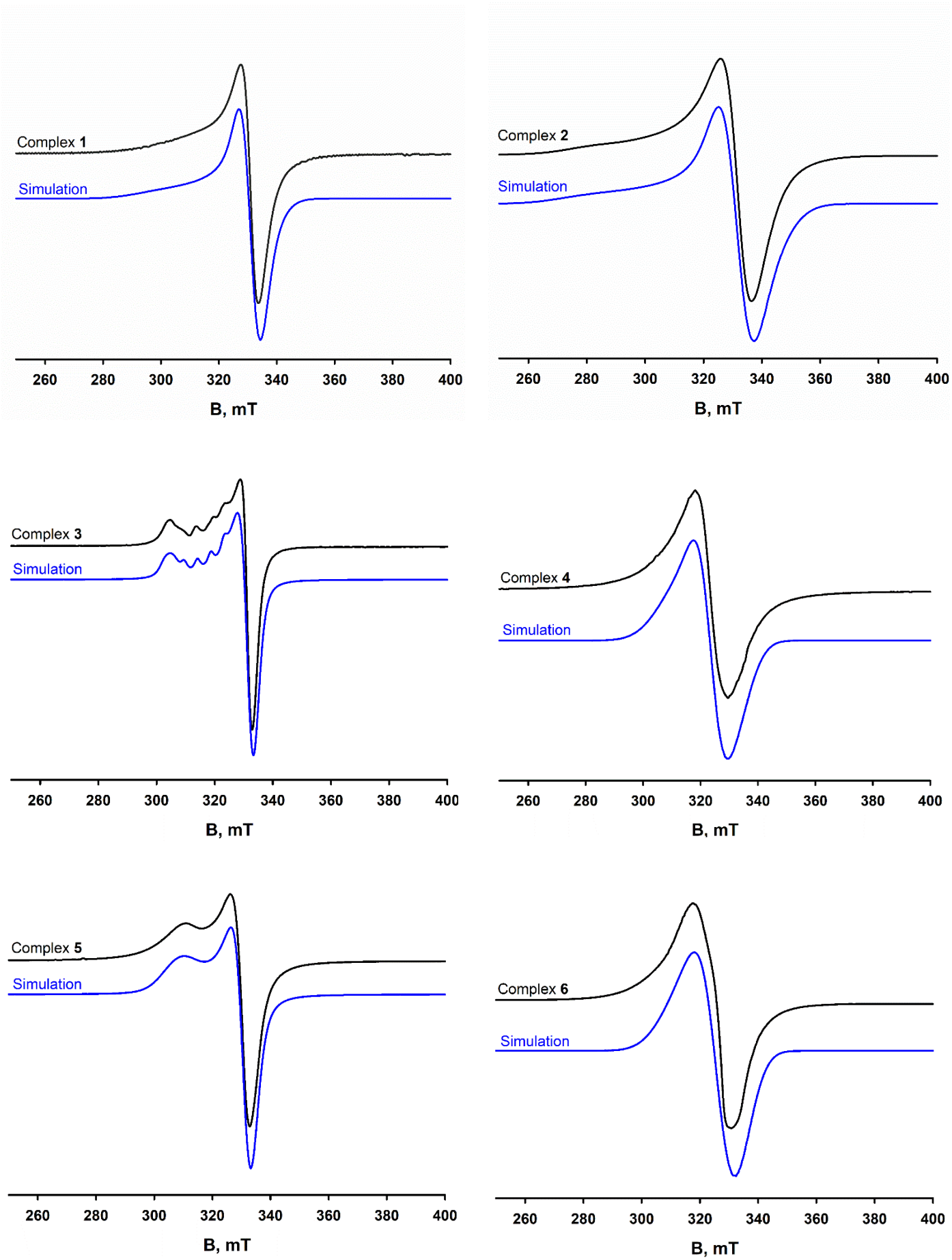

Figure S7. X-band EPR spectra of the polycrystalline samples of complex **1-6** at 77K. Spectrometer settings: microwave frequency 9.5 GHz, microwave power 2 mW.

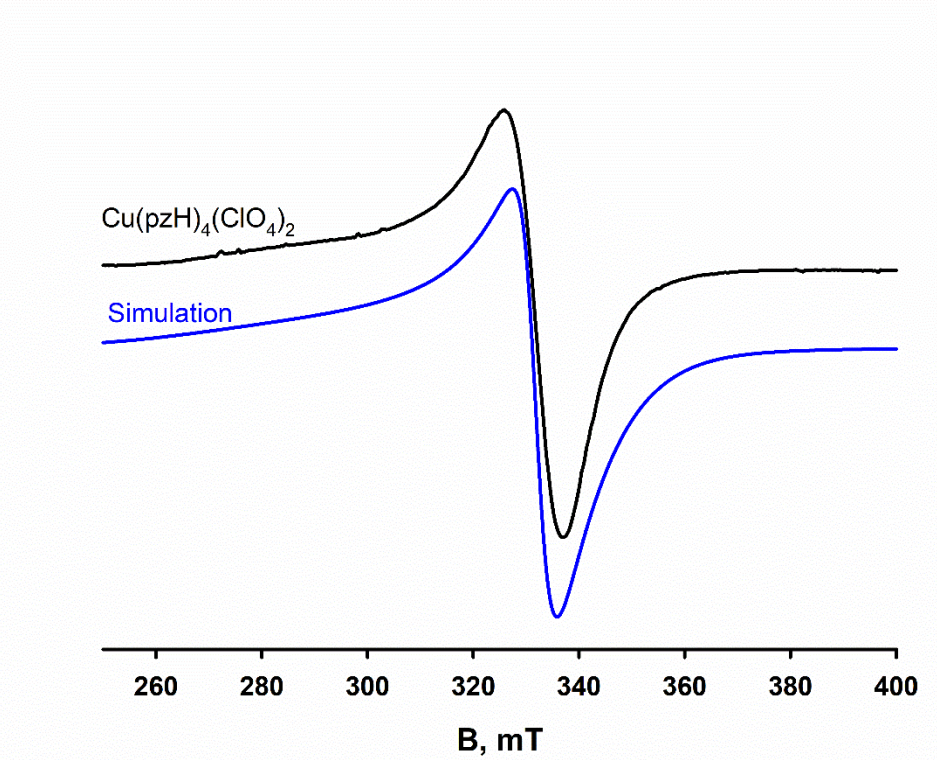

Figure S8. X-band EPR spectrum of the polycrystalline samples of complex $[Cu(pzH)_4(ClO_4)_2]$ at 77K. Spectrometer settings: microwave frequency 9.5 GHz, microwave power 2 mW.

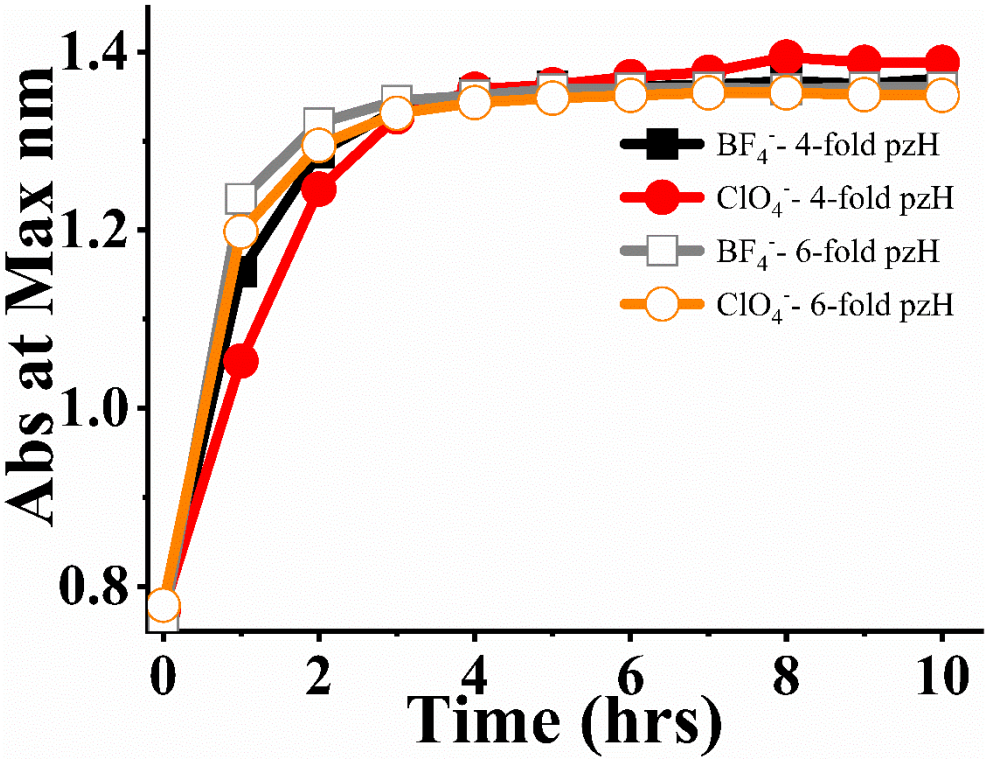

Figure S9. Time-dependent changes in the UV-vis spectrum from 0 to 10 hrs at 298 K for the formation of $[Cu(HN{=}C(Me)pz)_2(pzH)_2]^{2+}$ species, **1a**, from $Cu(ClO_4)_2{\cdot}6H_2O$ or $Cu(BF_4)_2$ (20 mM) and pzH in MeCN. The reactions were monitored by following the increasing absorption at 644 nm.

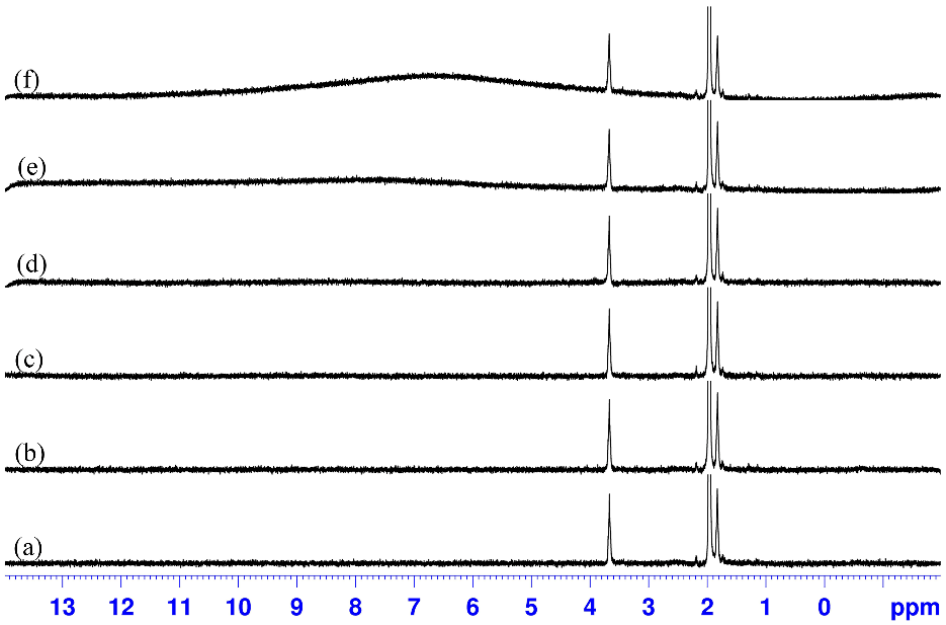

Figure S10. *In-situ* time-dependent ^1H NMR studies of $[Cu(pzH)_4(ClO_4)_2]$ dissolved in CD_3CN (1.95 ppm) at 298 K, (a) 5 mins, (b) 1 hr, (c) 2 hrs, (d) 4 hrs, (e) 6 hrs, (f) 9 hrs. The peaks at 1.7 and 3.6 ppm are belong to THF.

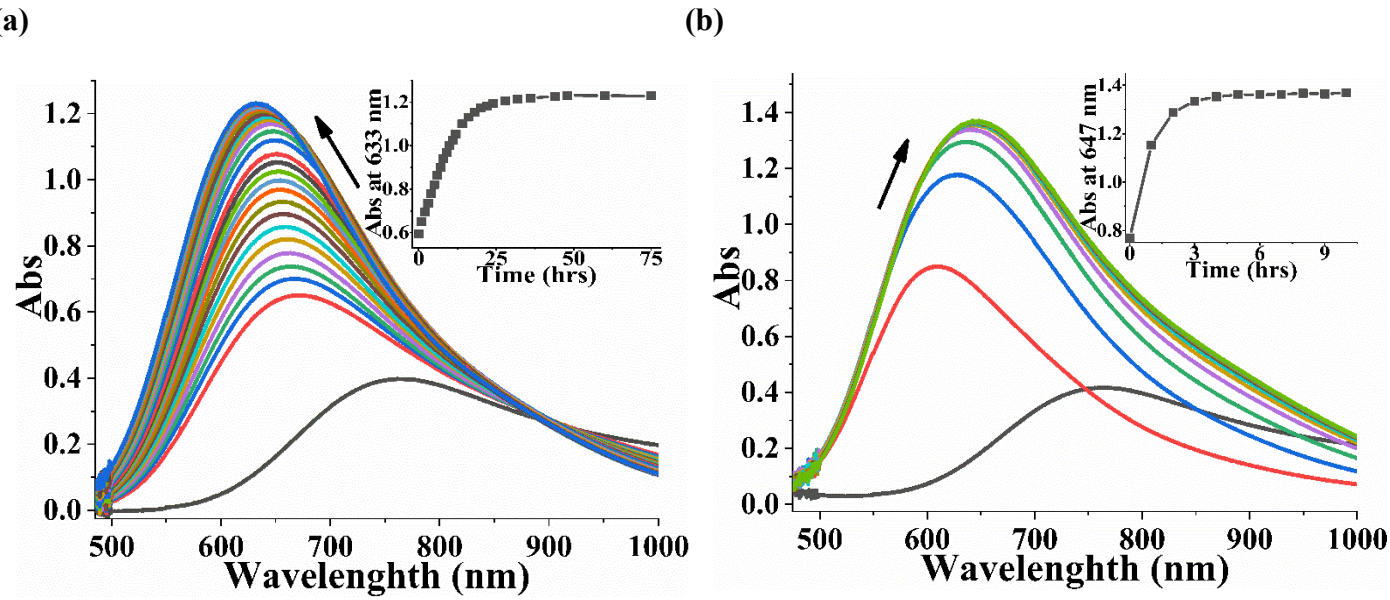

Figure S11. Time-dependent changes in the UV-vis spectrum from 0 to 75 hrs at 298 K for the formation of $[Cu(HN{=}C(Me)pz)_2(pzH)_2]^{2+}$ species from Cu(II) ion and pzH in MeCN. $Cu(BF_4)_2{\cdot}6H_2O$ (20 mM) was reacted with 2-fold (a) or 4-fold (b) excess of pzH in MeCN. The spectrum with absorption band maximum at 650 nm is corresponding to pure $Cu(ClO_4)_2{\cdot}6H_2O$ in MeCN. The reactions were monitored by following the increasing absorption at 633 or 647 nm (insets).

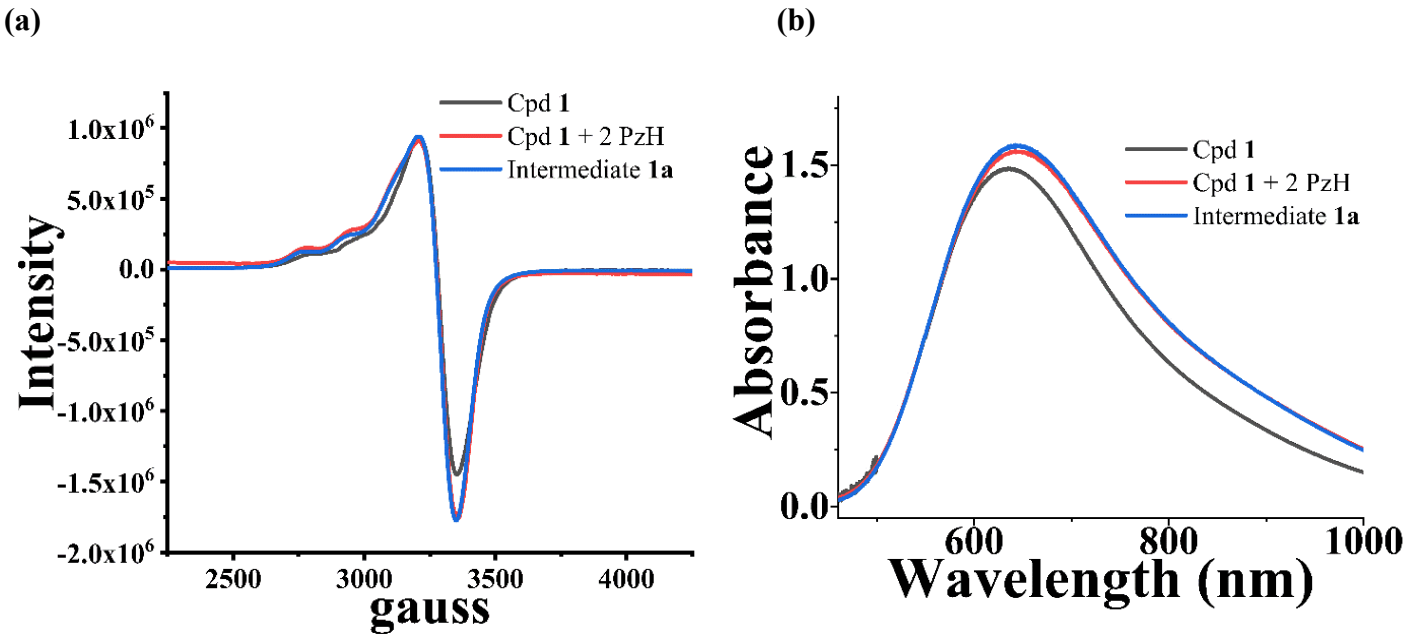

Figure S12. (a) X-band EPR spectra at 77K of complex **1** in MeCN (black line), complex **1** added with 2-fold pzH in MeCN (red line), and intermediate **1a** from the reaction of $Cu(ClO_4)_2$ with 4-fold pzH in MeCN (blue line). Spectrometer settings: microwave frequency 9.505 GHz, microwave power 2 mW. (b) UV-vis spectra of complex **1** in MeCN (blue line), complex **1** added with 2-fold pzH in MeCN (red line), and **1a** from $Cu(ClO_4)_2$ reacted with 4-fold pzH in MeCN (blue line) at 298 K.

(a) **(b)**

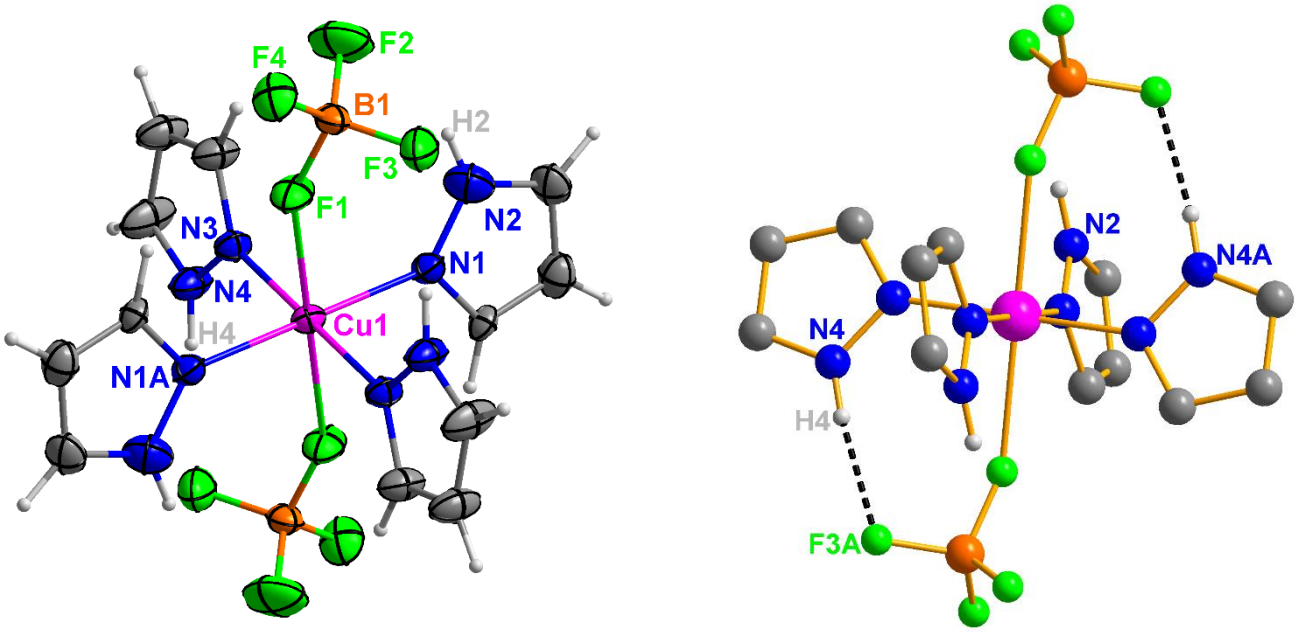

Figure S13. The Cu(II) ion in $[Cu(pzH)_4(BF_4)_2]$ lies on a crystallographic inversion center. (a) ORTEP drawings of $[Cu(pzH)_4(BF_4)_2]$. Thermal ellipsoids are drawn at the 35 % probability level. Selected bond lengths [Å] and angles [°]: Cu1-N1 2.008(2), Cu1-N3 1.990(2), Cu1-F1 2.3888(16), N1-Cu1-N3 90.02(9), N1-Cu1-N3A 89.98(9), N1-Cu1-F1 94.45(8), N3-Cu1-F1 90.17(8). (b) Balls and sticks representation of $[Cu(pzH)_4(BF_4)_2]$ with black dash lines showing the intramolecular NH···F hydrogen-bond interactions. No obvious intermolecular NH···F hydrogen-bond interactions was observed. Hydrogen bonding interactions: N4···F3A 2.9426(30) Å, H4···F3A 2.0690(18) Å, N4-H4···F3A 171.9(2)°. Symmetry code: A 0.5-x, 0.5-y, -z.